

## Structural and electronic properties of Au on TiO<sub>2</sub>(110)

Zongxian Yang and Ruqian Wu

*Department of Physics, California State University, Northridge, California 91330-8268*

D. W. Goodman

*Department of Chemistry, Texas A&M University, College Station, Texas 77843-3255*

(Received 18 October 1999)

The structure and electronic properties of 1-ML Au supported on TiO<sub>2</sub>(110) have been theoretically investigated using the full potential linearized augmented plane-wave method. Based on total-energy and atomic-force calculations, the preferential adsorption site for the Au adatom is predicted to be the atop site above the fivefold surface Ti atom, with a bond length of  $d_{\text{Au-Ti}}=2.66 \text{ \AA}$  and an adsorption energy of  $-1.49 \text{ eV}$  per adatom. The adsorption of Au enhances the binding energies of the valence bands and core levels of the surface Ti and O atoms, the Au  $d$  bands are destabilized with metallic gap states appearing near the Fermi level. This Au-substrate interaction leads to a more active Au site for the Au/TiO<sub>2</sub>(110) system compared to the Au(001) surface, in agreement with recent experimental observations.

### I. INTRODUCTION

Metal-oxide systems, especially those involving TiO<sub>2</sub>, have recently received considerable attention because of their technological importance as photocatalysts, chemical sensors, and heterogeneous catalysts.<sup>1,2</sup> Accordingly the growth of various metals such as Cr, Fe, Cu, Hf, and Pt on TiO<sub>2</sub> has been investigated.<sup>3-8</sup> Although gold has long been considered to be catalytically inactive, recently it has become a subject of intensive research because of its demonstrated unusual catalytic properties when highly dispersed, i.e.,  $<10 \text{ nm}$  clusters. For example, the Au/TiO<sub>2</sub> system has been shown to exhibit excellent properties as a chemical gas sensor and catalyst for room-temperature CO oxidation.<sup>9-11</sup> Highly dispersed Au on supports such as TiO<sub>2</sub> also exhibits an extraordinary high activity for low-temperature catalytic combustion and reduction of nitrogen oxides. Valden and co-workers<sup>12-15</sup> have studied in detail the structure and catalytic properties of Au on TiO<sub>2</sub> concluding that CO oxidation on Au/TiO<sub>2</sub>(110) is structure sensitive and that the unusual activity of the Au is likely due to quantum size effects in the highly dispersed Au clusters.

The adsorption and growth mode of Au on TiO<sub>2</sub>(110) within the submonolayer regime is a key to understanding the Au-TiO<sub>2</sub>(110) interfacial interaction and the unusual catalytic activity of supported Au. Zhang, Persaud, and Madey<sup>16</sup> have studied the growth of Au on TiO<sub>2</sub>(001) using low-energy ion scattering, x-ray photoelectron spectroscopy XPS, and low-energy electron diffraction and found that initially Au grows quasi-two-dimensionally (2D). No evidence of a significant chemical interaction was found between the Au adlayer and the TiO<sub>2</sub> substrate. Using the full potential-linear muffin-tin orbital (FP-LMTO) method, the electronic structure of  $5d$  transition metals (Ta to Au) on an unrelaxed TiO<sub>2</sub>(110) surface was studied by Thiên-Nga and Paxton<sup>17</sup> considering only one adsorption site (the atop site above the fivefold titanium surface atom). However, it is known that the TiO<sub>2</sub>(110) is significantly reconstructed;<sup>18,19</sup> therefore the actual Au adsorption site on the relaxed surface could differ

considerably from the unrelaxed surface. Thus it is important to consider the role of the substrate relaxations in altering the adsorption site and electronic properties of Au on TiO<sub>2</sub>(110).

In this paper, the full potential linearized augmented plane-wave (FLAPW) method<sup>20</sup> was used to study the adsorption of 1-ML Au on the relaxed TiO<sub>2</sub>(110). It is found that the Au adatoms prefer the atop site above the fivefold surface Ti atom, with a bond length of  $d_{\text{Au-Ti}}=2.66 \text{ \AA}$  and an adsorption energy of  $-1.49 \text{ eV}$  per adatom. The chemical properties of an Au site in Au/TiO<sub>2</sub>(110) appear to be very different from those in Au(001). The Au  $d$  band in Au/TiO<sub>2</sub>(110) is very close to the Fermi level ( $E_f$ ) and metallic states appear within the TiO<sub>2</sub> band gap, leading to the enhanced chemical reactivity of the Au/TiO<sub>2</sub>(110) system.

A brief description of the model and computational method is first presented, followed by first-principles results and discussion of bulk TiO<sub>2</sub>, the bare TiO<sub>2</sub>(110) surface, and the Au/TiO<sub>2</sub>(110) system.

### II. THE MODEL AND COMPUTATIONAL METHOD

The film version FLAPW method<sup>20</sup> has no shape approximation for charge, potential, and wave functions in the muffin-tin, interstitial, and vacuum regions. The local-density approximation (LDA) formalism of Hedin and Lundqvist<sup>21</sup> was used to describe the exchange-correlation potential and energy.

In the muffin-tin region, spherical harmonics with a maximum angular momentum of 8 are used to expand the charge, potential, and wave functions. In the interstitial region, plane waves with energy cutoffs of 324 Ry (for the charge and potential) and 16 Ry (for the variational bases) were employed. The Ti  $3p3d4s$  and O  $2s2p$  states were treated as valence states. The equilibrium structures were determined using total-energy and atomic forces,<sup>22</sup> with a criterion that required the force on each atom to be less than  $2 \times 10^{-3} \text{ hartree/a.u.}$  Sixteen  $k$  points in the irreducible part of the two-dimensional Brillouin zone [for the TiO<sub>2</sub>(110) clean surface and the Au/TiO<sub>2</sub>(110) systems] were used for the

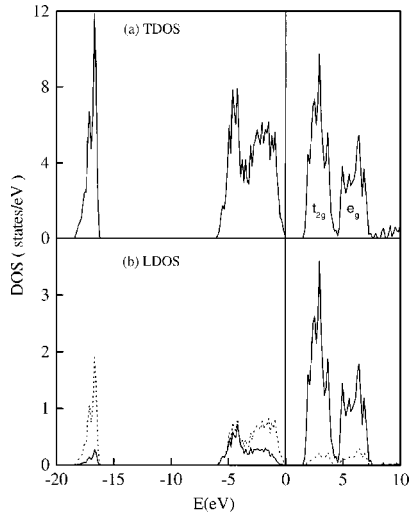


FIG. 1. The total (TDOS) (a) and local (b) density of states (LDOS) of the bulk  $\text{TiO}_2$ . The solid and dotted lines in panel (b) represent the LDOS of Ti and O, respectively. The solid vertical line at zero denotes the Fermi level.

integrals in reciprocal space. Test calculations for bulk  $\text{TiO}_2$  and clean  $\text{TiO}_2(110)$  surface with larger energy cutoffs showed that this approach is reasonable.

### III. BULK $\text{TiO}_2$ AND THE $\text{TiO}_2(110)$ CLEAN SURFACE

For bulk  $\text{TiO}_2$ , isotropic compressibility was assumed, i.e., the internal structural parameter  $u$  remains constant (0.305), and  $a$  and  $c$  scale isotropically. LDA calculations show that the total energy reaches its minimum at the experimental observed lattice constant values:<sup>23</sup>  $a = 4.594 \text{ \AA}$  and  $c = 2.952 \text{ \AA}$ . The calculated bulk modulus  $B$  is 228 GPa, very close to the experimental observed value (239 GPa).<sup>24</sup> In contrast, the calculated lattice constant using the generalized gradient approximation<sup>25</sup> (GGA) was found to be 2% larger than the experimental value.<sup>23</sup> Since the LDA method is known to describe Au better than GGA, LDA was used in the present studies. The calculated total and local density of states (DOS) for bulk  $\text{TiO}_2$  in the equilibrium geometry are shown in Fig. 1. The states from higher to lower stability have O  $2s$  (–18 to –16 eV), O  $2p$  (–6 to 0 eV), and Ti  $3d$  (2 to 7.5 eV) character, respectively.

$\text{TiO}_2$  is an insulator with a LDA-predicted band gap of 1.8 eV, a value smaller than the experimental value of 3.0 eV for well-known reasons.<sup>23</sup> Noting the local DOS (LDOS) in panel (b), it is apparent that the uppermost valence states consist primarily of the O  $2p$  component, while the Ti  $3d$  component dominates the conduction band. There is obvious hybridization between the Ti  $3d$  and the O  $2p$  states, especially in the energy range –6 to 0 eV. The Ti  $3d$  bands are separated into  $t_{2g}$  and  $e_g$  subbands because of the strong octahedral crystal field. These results agree well with Paxton's FP-LMTO data.<sup>26</sup>

The  $\text{TiO}_2(110)$  surface is the most thermodynamically stable  $\text{TiO}_2$  surface, and has been studied extensively by various experimental<sup>18,27–30</sup> and theoretical<sup>19,26,31–33</sup> methods. Using surface x-ray diffraction, the atomic relaxation of the  $\text{TiO}_2(110)-(1 \times 1)$  surface was studied by Charlton

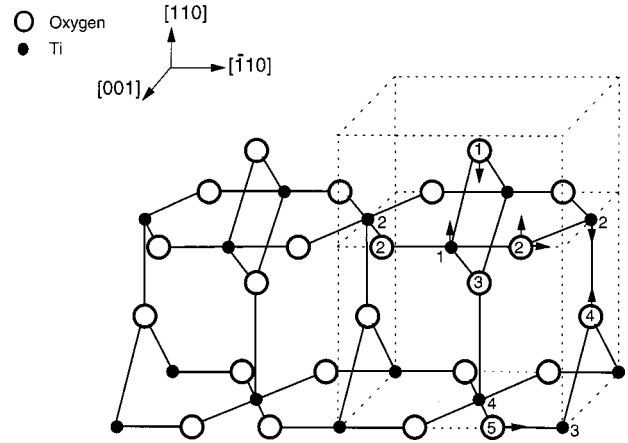


FIG. 2. The schematic geometry of the bulk-terminated  $\text{TiO}_2(110)-(1 \times 1)$  (only the upper half of the three-layer slab is drawn; the part in the dashed-line box is the upper-half unit cell used in our calculations). Small solid circles represent Ti and large open circles are for O.

*et al.*<sup>18</sup> The observed large surface relaxations, up to 0.27  $\text{\AA}$ , agree with *ab initio* pseudopotential total-energy calculations<sup>19</sup> especially for the positions of the surface titanium atoms.

In the present study the  $\text{TiO}_2(110)$  substrate is modeled by a three-layer slab shown in Fig. 2 (only the upper half of the slab is shown). The atoms in the model are fully relaxed according to their atomic forces; however, the in-plane symmetry in the 2D unit cell obtained from the ideally terminated rutile (110) surface is preserved. The calculated atomic displacements from their positions in the ideally terminated structure of  $\text{TiO}_2(110)-(1 \times 1)$  are listed in Table I, along with previous experimental<sup>18</sup> and theoretical (*ab initio* pseudopotential method) results.<sup>19</sup> The major relaxations occur along the surface normal with the fivefold Ti [denoted as  $T(2)$ ] and the sixfold Ti [denoted as  $\text{Ti}(1)$ ] moving inward and outward by 0.15 and 0.13  $\text{\AA}$ , respectively. The bridging oxygen [denoted as  $\text{O}(1)$ ] and the in-plane oxygen [denoted as  $\text{O}(2)$ ] move inward and outward by  $\sim 0.06$  and 0.13  $\text{\AA}$ , respectively. The  $\text{O}(2)$  and  $\text{O}(5)$  atoms relax laterally by 0.06 and 0.05  $\text{\AA}$ , respectively, along the  $[\bar{1}10]$  direction as indicated in Fig. 2. The relaxed  $\text{TiO}_2(110)$  is found to be puckered, agreeing well with earlier theoretical results for a five-layer slab<sup>19</sup> as well as with x-ray diffraction data.<sup>18</sup> Note that, for  $\text{O}(1)$ , a large discrepancy still exists between our theory and the x-ray diffraction result<sup>18</sup> ( $-0.06 \text{ \AA}$  vs  $-0.27 \pm 0.08 \text{ \AA}$ ). To check the possibility of local minimum or existence of metastable state, we carry out calculations using the experimental position<sup>18</sup> for  $\text{O}(1)$ . As a result, this structure gives a much higher total energy (by 0.67 eV/cell) than does the theoretically optimized structure for the clean  $\text{TiO}_2(110)$  surface.

The total density of states (TDOS) of the slab and the LDOS of the surface atoms for the relaxed  $\text{TiO}_2(110)$  surface are shown in Fig. 3. It is noteworthy that the band gap of the surface layer is reduced by 0.8 eV relative to the bulk crystal, and that an electrostatic shift occurs between the fivefold and sixfold Ti atoms. The DOS features of the  $\text{O}(1)$   $2s$  states are destabilized by approximately 1 eV relative to the  $\text{O}(2)$   $2s$

TABLE I. The calculated atomic displacements of Ti and O atoms from the ideally terminated structure of  $\text{TiO}_2(110)-(1 \times 1)$  for the clean and Au adsorbed  $\text{TiO}_2(110)$  systems, accompanied by the earlier experimental (Ref. 18) and theoretical [*ab initio* pseudopotential (p.p.) method] (Ref. 19) results of the clean surface. A negative (positive) value indicates that atoms move toward (away from) the surface for the perpendicular displacement. The  $\parallel$  denotes the movements along  $[\bar{1}10]$  direction for a lateral displacement. The actual directions of the movement are shown by arrows in Fig. 2. An asterisk indicates that the atom position was frozen in the calculation.

Atom type	Displacement ( $\text{\AA}$ )				
	Clean $\text{TiO}_2(110)$			Au/ $\text{TiO}_2(110)$	
	Expt. (Ref. 18)	p.p. method (Ref. 19)	Present	A site	C site
Ti(1)	$0.12 \pm 0.05$	0.13	0.13	0.11	0.11
Ti(2)	$-0.16 \pm 0.05$	-0.17	-0.15	-0.14	-0.10
Ti(3)	$-0.09 \pm 0.04$	-0.08	0.00	0.00	0.00
Ti(4)	$0.07 \pm 0.04$	0.07	0.00	0.00	0.00
O(1)	$-0.27 \pm 0.08$	-0.07	-0.06	-0.05	-0.06
O(2)[110]	$0.05 \pm 0.05$	0.13	0.13	0.08	0.10
O(2)[ $\bar{1}10$ ] $\parallel$	$-0.16 \pm 0.08$	*	-0.06	-0.04	-0.06
O(3)	$0.05 \pm 0.08$	-0.08	-0.05	-0.04	-0.05
O(4)	$0.00 \pm 0.08$	0.02	-0.004	-0.003	0.02
O(5)[110]	$0.02 \pm 0.06$	-0.03	0.00	0.00	0.00
O(5)[ $\bar{1}10$ ] $\parallel$	$-0.07 \pm 0.06$	*	-0.06	-0.03	-0.05

states. Satellite surface state features, also found by Paxton and Thiên-Nga,<sup>26</sup> appear at the bottom of the conduction band.

#### IV. THE ADSORPTION OF GOLD

The adsorption of 1 ML (one Au atom per surface unit cell) of Au atoms on the relaxed  $\text{TiO}_2(110)$  surface was studied by placing an Au adatom on each side of the relaxed  $\text{TiO}_2(110)$  slab. Three possible adsorption sites, *A* (on top of the fivefold Ti), *B* (on top of the sixfold Ti), and *C* (above the bridge of two in-plane O atoms along the  $[\bar{1}10]$  direction), shown in Fig. 4, were considered. The positions of the

adsorbed Au and the substrate atoms were optimized according to their atomic forces. The adsorption energies [defined as  $E_{\text{ad}} = \frac{1}{2}(E_{\text{Au/TiO}_2} - E_{\text{TiO}_2} - 2E_{\text{Au}})$ , with  $E_{\text{Au/TiO}_2}$ ,  $E_{\text{TiO}_2}$ , and  $E_{\text{Au}}$  representing the total energies of the adsorbed system, the clean  $\text{TiO}_2(110)$  surface, and a free Au monolayer, respectively] were  $-1.49$  eV/atom,  $-1.00$  eV/atom, and  $-1.41$  eV/atom for the three adsorption geometries (*A*, *B*, *C*), respectively. Overall, these adsorption energies are less than comparable values for metal/metal systems, but larger than those values found for metals adsorbed on  $\text{MgO}(001)$ .<sup>34</sup> In contrast, an unreasonably large adsorption energy ( $\sim 8.5$  eV/atom) for the broken row adsorption (corresponding to 0.5 ML Au) was found by Thiên-Nga and Paxton from their FP-LMTO calculations for Au adsorption on the unrelaxed  $\text{TiO}_2(110)$  surface.<sup>17</sup> Comparatively, the least favorable adsorption site is *B*, where the adsorption energy is only  $-1.0$  eV/atom. The *A* site is probably the most favorable adsorption site, followed closely by the *C* site ( $-1.49$  eV/adatom and  $-1.41$  eV/adatom, respectively). Obviously at elevated temperatures, i.e., a few hundred Kelvin, adsorption on either *A* and *C* sites is likely. The Au results are very similar to

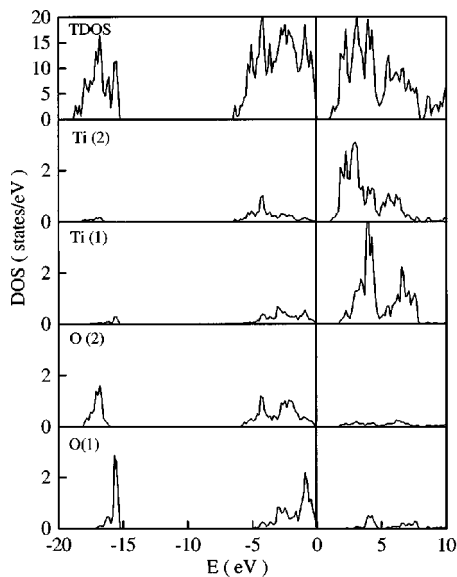


FIG. 3. The TDOS and LDOS of the  $\text{TiO}_2(110)$  clean surface. The solid vertical line at zero denotes the Fermi level.

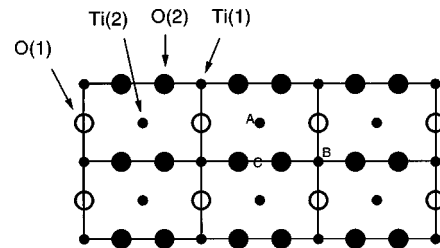
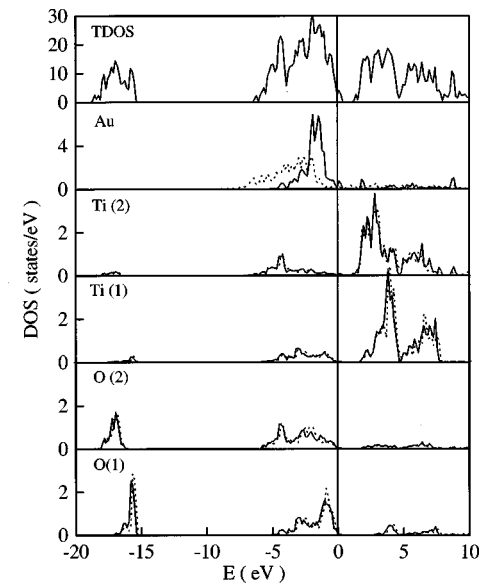
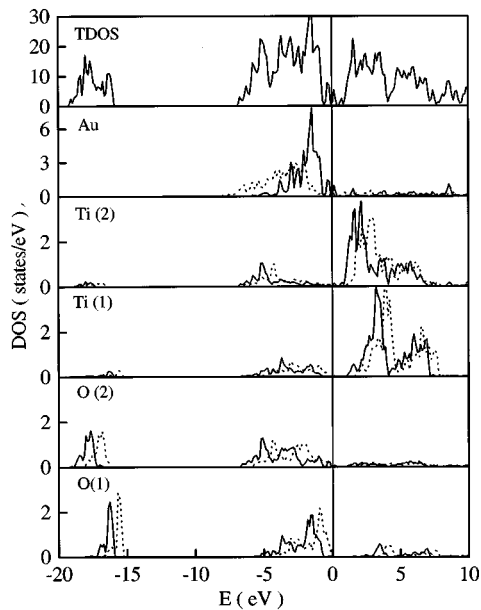


FIG. 4. Schematic geometry (top view) of the  $\text{TiO}_2(110)$  surface, with three possible adsorption sites considered in our studies marked as *A*, *B*, and *C*, respectively. The small solid circles represent the surface Ti, the large solid and open circles represent the in-plane O [O(2)] and the bridge O [O(1)], respectively.



(a)



(b)

FIG. 5. The TDOS and LDOS of the Au/TiO<sub>2</sub>(110) system for (a) A-site adsorption and (b) C-site adsorption. The dotted lines represent the LDOS for the Au(001) and TiO<sub>2</sub>(110) clean surfaces. The solid vertical line at zero denotes the Fermi level.

those found for Pt and Pd on TiO<sub>2</sub>(110), although both Pt and Pd have a greater preference for the A site.<sup>35,36</sup>

The atomic displacements from the ideally terminated structure of TiO<sub>2</sub>(110)-(1×1) in the equilibrium structures of the A and C adsorption sites of Au/TiO<sub>2</sub>(110) are shown in Table I. The adsorption of Au only slightly alters the relaxation of the TiO<sub>2</sub> substrate, even for the nearest-neighbor Ti and O atoms. On the A site, Au causes the nearest-neighbor O(2) to move inward by ~0.05 Å; Ti(1) also moves inward by 0.02 Å accompanied by a shift of the O(2). The bond lengths between the Au adatom and its nearest neighbors,

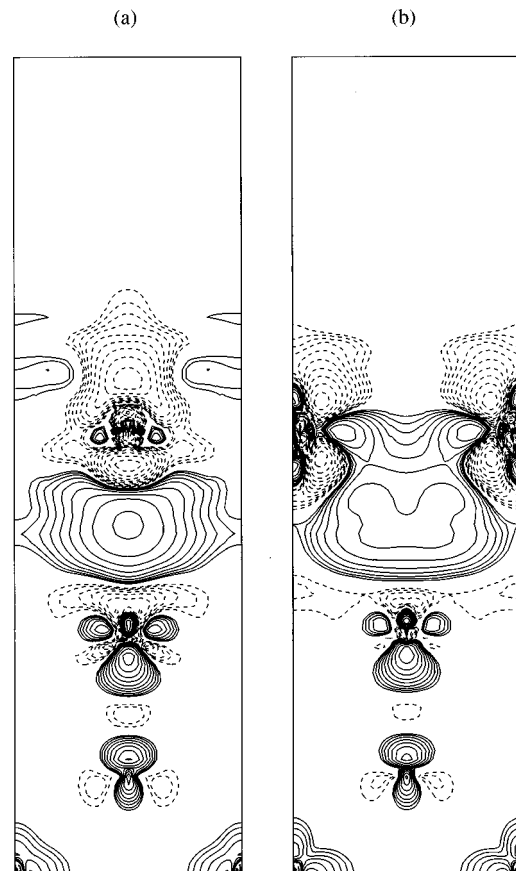


FIG. 6. The calculated charge density difference obtained by subtracting the superposition of the charge densities of Au monolayer and TiO<sub>2</sub>(110) from that of Au/TiO<sub>2</sub>(110) (a) for A-site adsorption, (b) for C-site adsorption. Contours are shown in the vertical (110) plane and start from  $1 \times 10^{-3}$  e/a.u.<sup>2</sup>, and increase successively by a factor of  $\sqrt{2}$ . Dashed lines indicate negative differences.

Ti(2) and O(2), are 2.66 and 3.11 Å, respectively. In contrast, with total-energy minimization for the unrelaxed TiO<sub>2</sub>(110) surface, a shorter Au-Ti(2) bond length (2.57 Å) was reported by Thiên-Nga and Paxton.<sup>17</sup> For Au adatoms on the C site, the nearest-neighbor Ti(2) [O(2)] atoms move outward (inward) by 0.05 Å (0.03 Å) from its corresponding position within the TiO<sub>2</sub>(110) clean surface. The Ti(1) site also shifts inward by 0.02 Å because of the change of the O(2) position. On the C site, the bond lengths between the Au adatom and its nearest Ti(2) and O(2) atoms are 2.95 and 2.65 Å, respectively.

The TDOS and LDOS for Au adsorption on the A and C sites are shown in Figs. 5(a) and 5(b), respectively. In Fig. 5(a), compared to the DOS of the TiO<sub>2</sub>(110) clean surfaces, Au adsorption on the A site induces no substantial change for the Ti and O sites. On the other hand, the Au *d* bands are now very close to  $E_f$ , which are mainly in the energy range of -5 to 0 eV, with a small feature lying just above the Fermi energy [i.e., a metal-induced gap state (MIGS)]. As discussed below, this is caused by charge polarization in the interfacial region and a subsequent increase of the potential in the adlayer. Such a large energy shift of the Au 5*d* band toward the  $E_F$ , as discussed by Hammer and Norskov,<sup>37</sup> and

TABLE II. The binding energies of the core states with respect to the Fermi level (in eV,  $4f_{7/2}$  for Au,  $2p_{3/2}$  for Ti and  $1s_{1/2}$  for O) for the Au/TiO<sub>2</sub> (110) systems in the *A*- and *C*-site cases. Results of relaxed (unrelaxed) TiO<sub>2</sub> (110) and Au (001) clean surfaces are also given.

Atom	Au on <i>A</i> site	Au on <i>C</i> site	Clean surface
Au	75.08	74.67	76.20 (75.99)
Ti(2)	437.83	437.91	437.24 (438.23)
O(2)	503.47	503.58	502.75 (503.57)
O(1)	501.70	502.47	501.68 (501.53)

also the induced gap state are expected to strongly alter the surface chemical properties of Au/TiO<sub>2</sub>(110) from those of the Au(001) clean surface.

For Au adsorption on the *C* site, the TDOS curve in Fig. 5(b) show that the gap is filled by many MIGS's, resulting mainly from the interaction between the Au atom and the nearest Ti(2) and O(2) atoms. Another major feature in Fig. 5 is the adsorbate-induced band bending, which can be clearly seen from the downward shifts of the Ti(1) and O(1) bands from the Fermi level. This band bending was observed by Zhang, Persaud, and Madey.<sup>16</sup>

To investigate the bonding mechanisms, the charge density differences obtained by subtracting the superposition of charge densities of the Au monolayer and the TiO<sub>2</sub>(110) clean surface from that of Au/TiO<sub>2</sub>(110) are plotted in Fig. 6. For adsorption of Au on the *A* site, Fig. 6(a) shows that electrons deplete from both the interfacial Au and Ti(2) sites and accumulate in the region between them. This suggests the formation of covalent bonds between Au and Ti(2).

Comparatively, for the *C* site adsorption [Fig. 6(b)], more electrons deplete from the top of the Au adatom. Charge accumulations can be found in the Au adlayer along the [001] direction, which suggests the formation of a metallic bond in the Au adlayer. This feature corresponds to the states in the gap (MIGS's) [cf. the panels of TDOS and Au in Fig. 5(b)]. The pronounced charge polarization in the interfacial region is responsible for the metal-induced band bending shown in Fig. 5(b).

By referring to the core-level energies in Table II, it is found that the binding energies of the core levels of Ti and O are stabilized relative to the relaxed TiO<sub>2</sub>(110) clean surface. The Ti(2)  $2p_{3/2}$  and O(2)  $1s_{1/2}$  levels are shifted to higher binding energies by 0.59 eV (0.67 eV) and 0.72 eV (0.83 eV), respectively, for the *A* site (*C* site). The binding energies of the valence states are also stabilized [cf. Figs. 5(a) and 5(b)], especially for the *C* site. The charge depletion around these atoms is mainly responsible for these binding energy increases. Similar core-level shifts were observed via XPS by Zhang, Persaud, and Madey,<sup>16</sup> who found that the Ti  $2p$  and O  $1s$  core-level features shift to higher binding energies by  $\sim 0.1$ – $0.2$  eV.

For the Au adlayer, the Au  $4f_{7/2}$  levels are predicted to be destabilized (*lower* binding energy) by 1.1 and 1.5 eV for the *A* and *C* sites, respectively, relative to the Au  $4f_{7/2}$  levels for the Au(001) clean surface. The valence DOS of the Au adlayer also shifts toward  $E_f$  by  $\sim 1.8$  eV relative to the Au(001) clean surface. These parallel shifts for the valence

and core states suggest that these arise from interfacial charge polarization and the subsequent potential shift in the adlayer. Recent XPS data of Luo, Kim, and Goodman,<sup>38</sup> indicate that the Au  $4f$  core level shifts to *higher* binding energy (0.8 eV) relative to bulk Au as Au clusters on TiO<sub>2</sub> become highly dispersed. XPS data of Zhang, Persaud, and Madey,<sup>16</sup> also show that the Au  $4f$  feature for thin Au films (1.1 Å) on TiO<sub>2</sub> have higher core-level binding energies (0.4 eV) relative to thick Au films (52 Å). At first glance the higher Au  $4f_{7/2}$  binding energies appear contradictory to the theoretical predictions. However, it is noteworthy that the Au  $4f$  core-level shifts observed by Luo, Kim, and Goodman,<sup>38</sup> for Au clusters supported on SiO<sub>2</sub>, show a higher binding energy of 1.6 eV for highly dispersed clusters relative to bulk Au, an increase attributable to final-state effects due to finite cluster sizes. That the Au  $4f_{7/2}$  core level shifts are 0.8 eV *lower* for small clusters of Au on TiO<sub>2</sub>(110) compared to small clusters of Au on SiO<sub>2</sub> is consistent with there being an initial state contribution of  $\sim -1.0$  eV for small clusters of Au on TiO<sub>2</sub>(110), close to the value predicted by the calculations (1.1–1.5 eV).

From Table II, the binding energies of the core levels are found to be structure sensitive, with clear differences between the core levels of the relaxed and the unrelaxed TiO<sub>2</sub>(110) clean surfaces. Noticeable differences are also evident between the core levels for the *A* and *C* adsorption sites, suggesting that different adsorption sites may be distinguishable using XPS.

## V. SUMMARY

The structure and electronic properties of Au on TiO<sub>2</sub>(110) have been studied using the full potential linearized augmented plane-wave (FLAPW) method. First, the adsorption of Au leads to small changes in the atomic and electronic structure of TiO<sub>2</sub>. Second, total-energy and atomic-force calculations indicate two possible preferred adsorption sites (*A* and *C*) differing very slightly in energy (1.49 vs 1.41 eV). Third, the valence and core-level binding energies of the surface Ti and O are found to be stabilized, which is qualitatively observed experimentally. Finally, the Au  $4f$  core-level shifts are predicted to be lower by 1.1–1.5 eV compared to bulk Au, consistent with recent XPS measurements.<sup>38</sup> Due to the interfacial interaction and charge polarization, the Au *d* bands in Au/TiO<sub>2</sub>(110) are very near  $E_f$ , with numerous MIGS's induced within the band gap, which likely contributes substantially to the enhanced catalytic activity of Au/TiO<sub>2</sub>(110) compared to bulk Au.

## ACKNOWLEDGMENTS

Z.Y. would like to thank Dr. V.I. Gavrilenko for his help with the calculations. This work was supported by the U.S. Department of Energy, Office of Basic Energy Sciences, Division of Chemical Sciences [Grant No. DE-FG03-99ER14948 (Z.Y. and R.W.) and Grant No. DE-FG03-95ER14511 (D.W.G)] and by computing time from NERSC. The Parson's foundation is also gratefully acknowledged for providing financial support.

- <sup>1</sup>R. J. Lad, Surf. Rev. Lett. **12**, 109 (1995).
- <sup>2</sup>A. M. Azad, S. A. Akbar, S. G. Mhaisalkar, L. D. Birkefeld, and K. S. Goto, J. Electrochem. Soc. **139**, 3690 (1992).
- <sup>3</sup>J. M. Pan, B. L. Maschoff, U. Diebold, and T. E. Madey, Surf. Sci. **191**, 381 (1993).
- <sup>4</sup>U. Diebold and T. E. Madey, Surf. Sci. **331/333**, 845 (1995).
- <sup>5</sup>J. M. Pan and T. E. Madey, J. Vac. Sci. Technol. A **11**, 1667 (1993).
- <sup>6</sup>U. Diebold and T. E. Madey, Phys. Rev. B **47**, 3868 (1993).
- <sup>7</sup>H.-P. Steinrück, F. Pesty, L. Zhang, and T. E. Madey, Phys. Rev. B **51**, 2427 (1995).
- <sup>8</sup>J. M. Pan, U. Diebold, and T. E. Madey, Surf. Sci. **195**, 411 (1993).
- <sup>9</sup>T. Kobayashi, M. Haruta, H. Sano, and M. Nakane, Sens. Actuators **13**, 39 (1988).
- <sup>10</sup>S. D. Lin, M. Bollinger, and M. A. Vannice, Catal. Lett. **17**, 245 (1993).
- <sup>11</sup>S. Lin and M. A. Vannice, Catal. Lett. **10**, 47 (1991).
- <sup>12</sup>M. Valden, X. Lai, and D. W. Goodman, Science **281**, 1647 (1998).
- <sup>13</sup>M. Valden, S. Pak, X. Lai, and D. W. Goodman, Catal. Lett. **56**, 7 (1996).
- <sup>14</sup>D. R. Rainer and D. W. Goodman, J. Mol. Catal. A: Chem. **131**, 259 (1998).
- <sup>15</sup>X. Lai, T. P. St. Clair, M. Valden, and D. W. Goodman, Prog. Surf. Sci. **59**, 25 (1998).
- <sup>16</sup>L. Zhang, R. Persaud, and T. E. Madey, Phys. Rev. B **56**, 10 549 (1997).
- <sup>17</sup>L. Thiên-Nga and A. T. Paxton, Phys. Rev. B **58**, 13 233 (1998).
- <sup>18</sup>G. Charlton, P. B. Howes, C. L. Nicklin, P. Steadman, J. S. G. Taylor, C. A. Muryn, S. P. Harte, J. Merce, R. McGrath, D. Norma, T. S. Turner, and G. Thornton, Phys. Rev. Lett. **78**, 495 (1997).
- <sup>19</sup>M. Ramamoorthy, D. Vanderbilt, and R. D. King-Smith, Phys. Rev. B **49**, 16 721 (1994).
- <sup>20</sup>E. Wimmer, H. Krakauer, M. Weinert, and A. J. Freeman, Phys. Rev. B **24**, 864 (1981); M. Weinert, E. Wimmer, and A. J. Freeman, *ibid.* **26**, 4571 (1982), and references therein.
- <sup>21</sup>L. Hedin and S. Lundqvist, J. Phys. C **33**, 373 (1972).
- <sup>22</sup>J. M. Soler and A. R. Williams, Phys. Rev. B **40**, 1560 (1989); R. Yu, D. Singh, and H. Krakauer, *ibid.* **43**, 6411 (1992).
- <sup>23</sup>P. Vinet, J. Ferrante, J. R. Smith, and J. H. Hose, J. Phys.: Condens. Matter **19**, L467 (1986).
- <sup>24</sup>*CRC Handbook of Chemistry and Physics*, 77th ed., edited by D. Lide (CRC, Boca Raton, Florida, 1997).
- <sup>25</sup>J. P. Perdew, K. Burke, and Y. Wang, Phys. Rev. B **54**, 16 533 (1996).
- <sup>26</sup>A. T. Paxton and L. Thiên-Nga, Phys. Rev. B **57**, 1579 (1998).
- <sup>27</sup>U. Diebold, J. F. Anderson, K.-O. Ng, and D. Vanderbilt, Phys. Rev. Lett. **77**, 322 (1996).
- <sup>28</sup>Q. Guo, I. Cocks, and E. M. Williams, Phys. Rev. Lett. **77**, 3851 (1996).
- <sup>29</sup>C. L. Pang, S. A. Haycock, H. Raza, P. W. Murray, G. Thornton, O. Gülseren, R. James, and D. W. Bullett, Phys. Rev. B **58**, 1586 (1998).
- <sup>30</sup>R. A. Bennett, P. Stone, N. J. Price, and M. Bowker, Phys. Rev. Lett. **82**, 3831 (1999).
- <sup>31</sup>P. Reinhardt and B. A. Hess, Phys. Rev. B **50**, 12 015 (1994).
- <sup>32</sup>K.-O. Ng and D. Vanderbilt, Phys. Rev. B **56**, 10 544 (1997).
- <sup>33</sup>P. J. D. Lindan, N. M. Harrison, M. J. Gillan, and J. A. White, Phys. Rev. B **55**, 15 919 (1997).
- <sup>34</sup>R. Wu and A. J. Freeman, Phys. Rev. B **51**, 5408 (1995); C. Li, R. Wu, A. J. Freeman, and C. L. Fu, *ibid.* **48**, 8317 (1993).
- <sup>35</sup>K. D. Schierbaum, S. Fischer, M. C. Torquemada, J. L. De Segovia, E. Roman, and J. A. Martin-Gago, Surf. Sci. **345**, 261 (1996).
- <sup>36</sup>C. Xu, X. Lai, G. W. Zajac, and D. W. Goodman, Phys. Rev. B **56**, 13 464 (1997).
- <sup>37</sup>B. Hammer and J. K. Nørskov, Surf. Sci. **343**, 211 (1996).
- <sup>38</sup>K. Luo, D. Y. Kim, and D. W. Goodman (unpublished).